Uranium(VI) Chemistry in Strong Alkaline Solution: Speciation and Oxygen Exchange Mechanism

6 AUTHORS, INCLUDING:

Björn Drobot
Helmholtz-Zentrum Dresden-Rossendorf
6 PUBLICATIONS **27** CITATIONS

Satoru Tsushima
Helmholtz-Zentrum Dresden-Rossendorf
**69** PUBLICATIONS **1,152** CITATIONS

Uranium(VI) Chemistry in Strong Alkaline Solution: Speciation and Oxygen Exchange Mechanism

Henry Moll, André Rossberg, Robin Steudtner, Björn Drobot, Katharina Müller, and Satoru Tsushima*

Institute of Resource Ecology, Helmholtz−Zentrum Dresden−Rossendorf (HZDR), Bautzner Landstraße 400, Dresden 01328, Germany

Ⓢ Supporting Information

ABSTRACT: The mechanism by which oxygen bound in UO_2^{2+} exchanges with that from water under strong alkaline conditions remains a subject of controversy. Two recent NMR studies independently revealed that the key intermediate species is a binuclear uranyl(VI) hydroxide, presumably of the stoichiometry $[(UO_2(OH)_4^{2-})(UO_2(OH)_5^{3-})]$. The presence of $UO_2(OH)_5^{3-}$ in highly alkaline solution was postulated in earlier experimental studies, yet the species has been little characterized. Quantum-chemical calculations (DFT and MP2) show that hydrolysis of $UO_2(OH)_4^{2-}$ yields $UO_3(OH)_3^{3-}$ preferentially over $UO_2(OH)_5^{3-}$. X-ray absorption spectroscopy was used to study the uranium(VI) speciation in a highly alkaline solution supporting the existence of a species with three U−O bonds, as expected for $UO_3(OH)_3^{3-}$. Therefore, we explored the oxygen exchange pathway through the binuclear adduct $[(UO_2(OH)_4^{2-})(UO_3(OH)_3^{3-})]$ by quantum-chemical calculations. Assuming that the rate-dominating step is proton transfer between the oxygen atoms, the activation Gibbs energy for the intramolecular proton transfer within $[(UO_2(OH)_4^{2-})(UO_3(OH)_3^{3-})]$ at the B3LYP level was estimated to be 64.7 kJ mol^{-1}. This value is in good agreement with the activation energy for "yl"−oxygen exchange in $[(UO_2(OH)_4^{2-})(UO_2(OH)_5^{3-})]$ obtained from experiment by Szabó and Grenthe (*Inorg. Chem.* **2010**, *49*, 4928−4933), which is 60.8 ± 2.4 kJ mol^{-1}. Both the presence of $UO_3(OH)_3^{3-}$ and the scenario of an "yl"−oxygen exchange through a binuclear species in strong alkaline solution are supported by the present study.
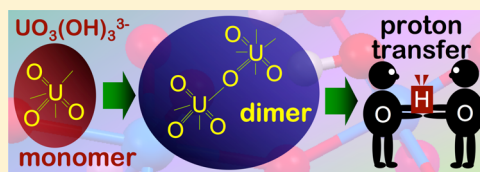
■ INTRODUCTION

The two axial oxygen atoms of the linear uranyl(VI) unit (so-called "yl"−oxygen atoms) have long been believed to be chemically inert until Clark et al. showed that they are rapidly exchangeable at high pH.[1] Later, Arnold et al. succeeded in covalent bond formation at one of the "yl"−oxygen atoms after uranium(VI) reduction to uranium(V).[2] Their work boosted research in that direction, and a significant amount of effort has been devoted to oxofunctionalization of uranyl(VI) complexes.[3] Yet there remains a fundamental open question regarding uranyl(VI) "yl"−oxygen, i.e., the mechanism of its exchange with oxygen in a highly alkaline aqueous solution. The uranyl(VI) "yl"−oxygen exchange takes place rather rapidly in alkaline solution, and it was first disputed whether or not $UO_2(OH)_n^{2-n}$ (n = 4 or 5) was the key species involved in the oxygen exchange.[1,4] From an NMR study,[1] it was suggested that $UO_2(OH)_n^{2-n}$ (n = 4 or 5) plays a key role in the oxygen exchange, although this model was refuted by density functional theory (DFT) calculations[4b] because the oxygen exchange within $UO_2(OH)_4^{2-}$ required an unrealistically high activation barrier.

In 2008, Shamov and Schreckenbach proposed a novel exchange pathway involving $UO_2(OH)_4^{2-}$, $UO_2(OH)_5^{3-}$, and $UO_3(OH)_3^{3-}$ based on DFT calculations.[5] They showed that the oxygen exchange takes place in $UO_2(OH)_n^{2-n}$ through the formation of a $UO_3(OH)_3^{3-}$ species. However, very recently Szabó and Grenthe[6] as well as Harley et al.[7] independently suggested that the oxygen exchange in alkaline solution takes

place via formation of a binuclear complex or a transition state which presumably has the stoichiometry $[(UO_2(OH)_4^{2-})-(UO_2(OH)_5^{3-})]$. The apparent contradiction between theory and experiment suggests that there is a need to study the dimer scenario computationally and in relation to the "Shamov−Schreckenbach complex" ($UO_3(OH)_3^{3-}$). Very recently, Clark et al. experimentally studied the "yl"−oxygen exchange in the neptunyl(VI) unit under strong alkaline condition and proposed a mechanism similar to the one in the uranyl(VI) system. However, Clark et al. did not discuss in detail the possible species involved in the "yl"−oxygen exchange.[8]

It is reasonable that the oxygen exchange of uranyl(VI) is facilitated by the formation of a binuclear complex. The exchange of the uranyl(VI) oxygen atoms in acidic media is known to take place via the formation of the binuclear species $(UO_2)_2(\mu_2\text{-}OH)_2^{2+}$.[4c,9] The entire pathway was thoroughly identified by B3LYP calculations.[10] The key step was found to be an U−O_{yl}−U bridge formation between the two uranyl(VI) centers.

The primary aim of this study is to identify the uranyl(VI) "yl"−oxygen exchange mechanism in the alkaline system using quantum-chemical methods with a focus on the binuclear scenario. For this attempt, it was essential to experimentally confirm (or otherwise refute) the presence of the yet undetected species $UO_3(OH)_3^{3-}$. Therefore, the aqueous

speciation of uranyl(VI) in a strong alkaline medium was experimentally investigated using X-ray absorption spectroscopy (XAS).

Reactions involving a new U–O bond formation or a change in the uranium coordination number require careful theoretical treatment because previous studies pointed out that reaction energies as well as reaction barriers may be over- or underestimated.[11] Therefore, a further issue is addressed in this article as well, i.e., the role of different DFT functionals for studying the oxygen exchange (namely, proton transfer) in uranyl(VI) hydroxides.

■ RESULTS AND DISCUSSION

Hydrolysis beyond $UO_2(OH)_4^{2-}$ Studied by Quantum-Chemical Calculations. Previously, Shamov and Schreckenbach proposed from a series of DFT calculations an oxygen-exchange pathway involving $UO_2(OH)_4^{2-}$, $UO_2(OH)_5^{3-}$, and $UO_3(OH)_3^{3-}$.[5] Here, we have investigated the equilibrium among these three complexes by DFT methods (M06-2X, B3LYP, and BP86) as well as by a Möller–Plesset second-order perturbation theory (MP2) approach. Scheme 1 illustrates the three complexes that have been studied.

Scheme 1. Equilibrium among 1–3[a]
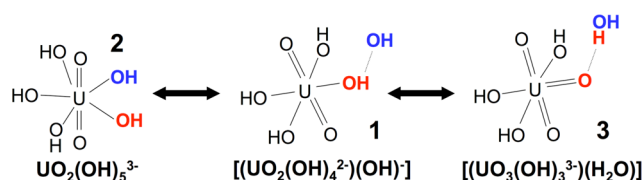
[a]The relative energy differences among these complexes at various levels of theory are given in Table 1.

First, the equilibrium between the tetrahydroxo ($[(UO_2(OH)_4^{2-})(OH)^-]$, **1**) and pentahydroxo species ($UO_2(OH)_5^{3-}$, **2**) was studied. The reaction energy and activation barrier are given in Table 1 (second to fourth

Table 1. Relative Gibbs Energy and Gibbs Energy of Activation of the Complexes in Scheme 1[a]

	2	TS[b]	1	TS[c]	3
M06-2X	+10.6	+46.9	0.0	+7.7	+19.4
B3LYP	+45.1	+65.1	0.0	+3.7	+17.6
BP86	+52.3	+59.2	0.0	−6.8	+3.5
MP2	+23.3	+55.3	0.0	+2.1	+1.0
MP2 with B3LYP geometry[d]	+18.7	+51.4	0.0	−0.5	−2.7

[a]The energy is relative to complex **1** in kJ mol^{-1}. [b]Transition state between **1** and **2**. [c]Transition state between **1** and **3**. [d]The Gibbs energy corrections were taken from the results at the B3LYP level.

columns). The relative energy differences of pentahydroxouranyl(VI) compared to the tetrahydroxo complex showed diverging results depending on the different methodologies. M06-2X gave the lowest energy of +10.6 kJ mol^{-1}, whereas BP86 gave the highest value of +52.3 kJ mol^{-1}. At the MP2 level, the energy was +23.3 kJ mol^{-1} for the same reaction. Compared to MP2, the reaction energy using the B3LYP and BP86 functionals was overestimated, whereas it was somewhat underestimated using M06-2X. This problem was pointed out previously,[11c,12] and several DFT functionals including B3LYP and BP86 were found to underestimate the

binding energies between the metal and ligand. In other words, the stability of uranyl(VI) complexes having higher uranium coordination number tends to be underestimated using these methods. When B3LYP or BP86 functionals were used, the reaction energy was overestimated (or underestimated) if the reaction involved an increase (or decrease) in the coordination number of uranium. This tendency, however, was not due to the deficiency of DFT, in general, but rather that of the functionals. When the M06-2X functional was used, the reaction energy was much lower for the equilibrium between **1** and **2** and it was closer to the energy at the MP2 level. The transition state between **1** and **2** was also identified at all levels of theory. The results are rather consistent with activation Gibbs energies between +46.9 and +65.1 kJ mol^{-1} (Table 1, third column). For the same reaction, Shamov and Schreckenbach obtained a much higher activation Gibbs energy of +89.1 kJ mol^{-1}.[5] The difference is that Shamov and Schreckenbach performed the calculations in the gas phase although the final energy included the solvation energy. In addition, the Perdew–Burke–Ernzerhof (PBE) functional was used in the study of Shamov and Schreckenbach.

Second, we have studied the equilibrium between **1** and ($[(UO_3(OH)_3^{3-})(H_2O)]$, **3**). The reaction energy and activation barrier are given in Table 1 (fourth to sixth columns). Again, the results depend strongly on the methodologies. The M06-2X and B3LYP functionals gave much higher energies than BP86, whereas the result at the BP86 level was close to that at the MP2 level. In the equilibrium between **1** and **3**, there was no change in the uranium coordination number but there was an oxo bond formation/deformation. Presumably, M06-2X and B3LYP underestimated the stability of uranium(VI) complexes having an increased number of oxo bonds. The activation energy between **1** and **3** ranged from −6.8 kJ mol^{-1} at the BP86 level to +7.7 kJ mol^{-1} at the M06-2X level. A small negative activation barrier is a computational artifact and not an indication of an error in computation, an issue that has been discussed elsewhere.[12b] At all levels of theory, the activation barrier was overall low, such that **1** can readily transform into **3**, implying that $UO_3(OH)_3^{3-}$ can be formed if there is sufficient concentration of the hydroxo anion. Therefore, in principle, the trioxo species $UO_3(OH)_3^{3-}$ can be formed to an appreciable amount if the pH of the uranyl(VI) solution is high enough.

Shamov and Schreckenbach assumed in their DFT study that **3** was formed by the stepwise reaction **1** → **2** → **3**. However, in the subsequent Car–Parrinello molecular dynamics (CPMD) study by Bühl and Schreckenbach,[11a] the authors concluded that **3** can be directly formed from **1** via deprotonation. In the present study, the activation energy as well as the reaction energy of **1** → **2** was found to be overall higher than that of **1** → **3**, and the direct formation of **3** from **1** was found to be more likely than that through **2**. Moreover, it was not possible to identify the transition state between **2** and **3** at all levels of the used theories. These results together with the CPMD results by Bühl and Schreckenbach suggested that $UO_3(OH)_3^{3-}$ can be formed directly from $UO_2(OH)_4^{2-}$ without the formation of $UO_2(OH)_5^{3-}$.

Previously, Clark et al.[1] and Moll et al.[13] found in a strongly alkaline uranyl(VI) solution a new complex in addition to $UO_2(OH)_4^{2-}$.[13] They concluded that the new species is $UO_2(OH)_5^{3-}$. In a more recent study, Quilès et al. confirmed this finding. In addition, they proposed a new complex that they assigned to a further hydrolyzed species $UO_2(OH)_6^{4-}$.[14]

The presence of hexahydroxouranyl(VI), however, could not be confirmed by DFT calculations. All attempts to optimize the structure of $UO_2(OH)_6^{4-}$ failed. Such a complex was found to be dissociative. The equatorial plane of the linear uranyl(VI) unit cannot accommodate six hydroxo ligands because in such a complex the neighboring OH^- ligands get too close. In the Raman spectra of Quilès et al., the ratio between $UO_2(OH)_5^{3-}$ and $UO_2(OH)_6^{4-}$ remained almost constant upon variation of the pH of the solution. This seems to be self-contradictory to their own assignment. We finally decided not to go deeper into this issue in the present manuscript. Nevertheless, the existence of species beyond $UO_2(OH)_4^{2-}$ is undoubted, and our calculations show that $UO_3(OH)_3^{3-}$ is preferred over $UO_2(OH)_5^{3-}$. The species identified as $UO_2(OH)_5^{3-}$ by the previous authors might be, in fact, $UO_3(OH)_3^{3-}$. According to Scheme 1, deprotonation to $UO_3(OH)_3^{3-}$ yields one water molecule whereas deprotonation to $UO_2(OH)_5^{3-}$ does not. This implies that when the concentration of water is low, such as in a methanol−water mixture or under very high pH, $UO_3(OH)_3^{3-}$ is even more preferred over $UO_2(OH)_5^{3-}$. Therefore, the predominance of $UO_3(OH)_3^{3-}$ in methanol compared to water, as evidenced by Moll et al.,[13] can be understood.

Hydrolysis beyond $UO_2(OH)_4^{2-}$ Studied by XAS. The quantum-chemical calculations described above suggest that hydrolysis of $UO_2(OH)_4^{2-}$ yields $UO_3(OH)_3^{3-}$ instead of $UO_2(OH)_5^{3-}$. In principle, the species $UO_2(OH)_5^{3-}$ and $UO_3(OH)_3^{3-}$ can be distinguished by Raman or IR spectroscopy, with the latter giving smaller frequencies for the symmetric and asymmetric stretching modes of the O=U=O oscillator. Quilès et al. obtained Raman spectra of the species beyond $UO_2(OH)_4^{2-}$. We have plotted their experimental results versus the theoretical O=U=O symmetric stretching frequency (Figure S1 in the Supporting Information, SI) assuming that the species found by Quilès et al. with a Raman active band at 767 cm^{-1} is either $UO_2(OH)_5^{3-}$ or $UO_3(OH)_3^{3-}$. Fitting the new species to $UO_3(OH)_3^{3-}$ results in an R^2 value of 0.998, very similar to the corresponding R^2 value of 0.999 obtained from fitting to $UO_2(OH)_5^{3-}$. Therefore, the Raman data by Quilès et al. neither confirmed nor disproved the presence of $UO_3(OH)_3^{3-}$.

To study this point further, two uranium(VI) samples were prepared in a strong alkaline solution (**S1** and **S5**) for spectroscopic investigation. **S1** contained 50 mM uranyl(VI) in a 1.0 M aqueous tetramethylammonium hydroxide (TMA-OH) solution. **S5** also contained 50 mM uranyl(VI) but in a 3.0 M TMA-OH methanol solution. It is clear from the previous studies that $UO_2(OH)_4^{2-}$ predominates in **S1**.[1,13,15] In **S5**, with a higher TMA-OH concentration, we expected the presence of the further hydrolyzed species $UO_2(OH)_5^{3-}$ or $UO_3(OH)_3^{3-}$. However, it is also likely that deprotonated methanol (MeO^-), instead of OH^-, could be partly coordinated to uranium. The resulting stoichiometry of the species can be described as $UO_2(MeO)_m(OH)_n^{2-}$ ($m + n = 4$, $m > 0$) and $UO_3(MeO)_k(OH)_l^{3-}$ ($k + l = 3$, $k > 0$). This is because methanol is only slightly more acidic than water so that MeO^- is abundant in highly alkaline methanol/water mixtures.

We measured U L_{III}-edge X-ray absorption near edge structure (XANES) spectra of these samples, and the results are shown in Figure 1. As was already mentioned, $UO_2(OH)_4^{2-}$ comprises nearly 100% of **S1**. In **S5**, there is probably a mixture of the species $UO_2(MeO)_m(OH)_n^{2-}$ and $UO_3(MeO)_k(OH)_l^{3-}$. In the previous NMR study by Moll et al., the authors used the
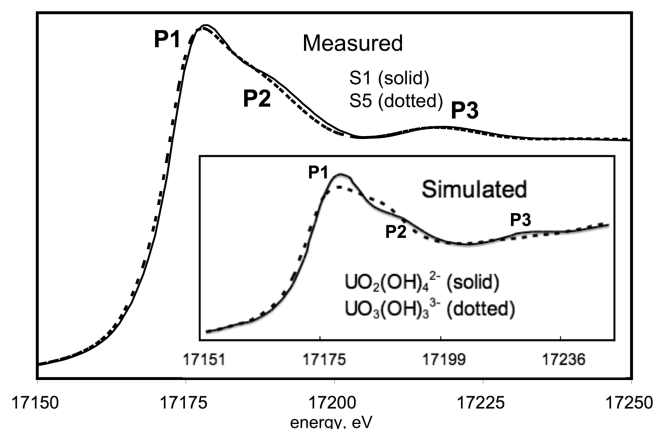
Figure 1. U L_{III}-edge XANES spectra of 50 mM uranyl(VI) in a 1.0 M TMA−OH aqueous solution at room temperature (sample **S1**) and in a 3.0 M TMA-OH methanol/water mixture at 200 K (sample **S5**). The inset shows the simulated spectra of $UO_2(OH)_4^{2-}$ and $UO_3(OH)_3^{3-}$ using the *FEFF9* program.

same solution as **S5**, but they measured the spectra at 258 K. Moll et al. concluded that the sample is a 3:1 mixture of $UO_2(OH)_4^{2-}$ and $UO_2(OH)_5^{3-}$, although we suspect here that it is a mixture of $UO_2(MeO)_m(OH)_n^{2-}$ ($m + n = 4$) and $UO_3(MeO)_k(OH)_l^{3-}$ ($k + l = 3$). In the present investigation, XAS measurements were performed at lower temperature (200 K) compared to those of Moll et al. (258 K), and the fraction of the further hydrolyzed species, namely, $UO_3(MeO)_k(OH)_l^{3-}$, must therefore be greater than 25% found by Moll et al. at 258 K because methanol has a significantly higher dielectric constant at lower temperature (approximately 50% higher at 200 K compared to that at 258 K). Correspondingly, the presence of the higher charged species is expected to be more pronounced under conditions of a higher dielectric constant. However, a prediction of the actual speciation is difficult because of a lack of thermodynamic data.

From Figure 1, it can be seen that the U L_{III} absorption edge (P1) of **S5** is slightly shifted to lower energy (~0.5 eV) compared to that of **S1**. Such a shift can be interpreted as uranium(VI) reduction to uranium(V) or uranium(IV). However, the samples were kept in the dark under a N$_2$ atmosphere immediately after the preparation to avoid photochemical redox reactions. Also, when **S5** was measured at room temperature, the energy shift was not observed. Therefore, the shift of P1 indicates a speciation change of uranium(VI) rather than a change in the oxidation state of uranium. In a previous study on protactinium(V) [which is isoelectronic to uranium(VI)] by Le Naour et al.,[16] the authors found a similar energy shift of the Pa L_{III} absorption edge in going from a spherical Pa^{5+} ion (in a HF solution) to a monooxo PaO^{3+} ion (in a H$_2$SO$_4$ solution). As demonstrated in the protactinium case by Le Naour et al., the formation of an additional oxo bond to the actinide center provokes a shift of the absorption edge; hence, the shift of the absorption edge on going from **S1** to **S5** is in accordance with our hypothesis that there is an additional oxo bond formation in the species in **S5**, namely, the formation of $UO_3(MeO)_k(OH)_l^{3-}$. To further confirm this hypothesis, we simulated the XANES spectra (U L_{III}-edge) of $UO_2(OH)_4^{2-}$ and $UO_3(OH)_3^{3-}$ molecules using the *FEFF9* program, as shown in the inset of Figure 1. The structures of $UO_2(OH)_4^{2-}$ and $UO_3(OH)_3^{3-}$ were taken from the B3LYP results. The simulations result in a slight shift (~1

eV) of the absorption edge (P1) of $UO_3(OH)_3^{3-}$ compared to $UO_2(OH)_4^{2-}$. Also, the shoulder P2 in $UO_2(OH)_4^{2-}$ is shifted to lower absorption energy in $UO_3(OH)_3^{3-}$, and the shoulder P3 in $UO_2(OH)_4^{2-}$ is not apparent in $UO_3(OH)_3^{3-}$. These two shoulders originate from multiple scattering paths of axial and equatorial oxygen atoms, respectively.[17] The overall features of the simulated XANES spectra of $UO_2(OH)_4^{2-}$ and $UO_3(OH)_3^{3-}$ match the measured spectra of S1 and S5, respectively, although the spectral differences are more pronounced in the simulated spectra than in the experimental ones. This is understood because $UO_2(MeO)_m(OH)_n^{2-}$ is still the predominating species in sample S5 and $UO_3(MeO)_k(OH)_l^{3-}$ contributes less.

We have also analyzed extended X-ray absorption fine structure (EXAFS) spectra of samples S1 and S5, which are given in Figure S2 in the SI. Extracted structural parameters are summarized in Table S1 in the SI. In the spectra of sample S1, we found two U−O distances of 1.82 and 2.27 Å assigned to the U−O_{ax} and U−O_{eq} bonds of $UO_2(OH)_4^{2-}$, respectively. Corresponding numbers in our B3LYP calculations are 1.83 and 2.28 Å, respectively, and EXAFS and DFT U−O distances are in excellent agreement. By contrast, the EXAFS spectrum of sample S5 does not provide convincing information because as mentioned above this sample is a mixture of $UO_2(MeO)_m(OH)_n^{2-}$ and $UO_3(MeO)_k(OH)_l^{3-}$, where the ratio of the species as well as the parameters m, n, k, and l all remain unidentified. If we take into account the existence of multiple species each comprised of multiple U−O distances, EXAFS analysis of S5 becomes far too complicated even with the help of factor analysis,[18] and we were not able to unequivocally extract more than two distinct species from the spectra of S5. However, when S5 was fitted with a single species with only two oxygen shells (U−O_{ax} and U−O_{eq}), we found a large Debye−Waller (DW) factor for U−O_{ax}, as shown in Table S1 in the SI. A large DW factor for the U−O_{ax} shell is unusual even when there is a mixing of multiple species. It should also be noted that S5 was measured at low temperature, which should, in principle, give a lower DW factor compared to S1. A large DW factor observed for the U−O_{ax} shell at low temperature was another evidence to support the presence of the species having three U−O oxo bonds.

Binuclear Complex Formation between $UO_2(OH)_4^{2-}$ and $UO_3(OH)_3^{3-}$ Studied by Quantum-Chemical Calculations. Szabó and Grenthe suggested that a binuclear complex or a transition state with the stoichiometry $[(UO_2(OH)_4^{2-})$-$(UO_2(OH)_5^{3-})]$ is likely to be responsible for the oxygen exchange in an alkaline aqueous solution.[6] Harley et al. supported the dimer scenario proposed by Szabó and Grenthe, but they could not derive information about the stoichiometry of the complex.[7] The probability of a binuclear complex formation of uranyl(VI) hydroxide was addressed by quantum-chemical calculations comparing the Gibbs energy of outer- and inner-sphere complexes of uranyl(VI) hydroxide dimers. If the inner-sphere complex is energetically stable enough compared to its outer-sphere counterpart, it can be concluded that the binuclear complex is likely to be formed.

DFT structure optimization and single-point MP2 energy calculations using B3LYP structures (B3LYP/MP2) were performed because geometry optimizations at the MP2 level were too costly for dimeric species. For the monomeric uranyl(VI) hydroxo species, we found a reaction energy difference between the pure MP2 and B3LYP/MP2 calculations to be less than 5 kJ mol^{-1} (Table 1, last two rows). However,

B3LYP/MP2 calculations tend to underestimate the reaction energies compared to the pure MP2 method. Shamov and Schreckenbach concluded from a series of quantum-chemical calculations on uranyl(VI) complexes that MP2 gives slightly worse energetics than hybrid functionals.[19] Finally, on the basis of previous works on uranyl(VI) "yl"−oxygen exchange independently performed by Bühl et al., Schreckenbach et al., and Tsushima,[5,10,11,12a] using hybrid DFT functionals, we conclude that B3LYP is one of the best compromises for studying the "yl"−oxygen exchange in uranyl(VI) species. The formation of $[(UO_2(OH)_4^{2-})(UO_2(OH)_5^{3-})]$, as suggested by Szabó and Grenthe, as well as the formation of the alternative species $[(UO_2(OH)_4^{2-})(UO_3(OH)_3^{3-})]$ has been investigated (Scheme 2). In the case of $[(UO_2(OH)_4^{2-})(UO_2(OH)_5^{3-})]$,

Scheme 2. Formation of Inner-Sphere Binuclear Complex with the Stoichiometry $[(UO_2(OH)_4^{2-})(UO_2(OH)_5^{3-})]$ (Upper, 5) and $[(UO_2(OH)_4^{2-})(UO_3(OH)_3^{3-})]$ (Lower, 7)[a]

$[(UO_2(OH)_4^{2-})(UO_2(OH)_5^{3-})]$

$[(UO_2(OH)_4^{2-})(UO_3(OH)_3^{3-})]$
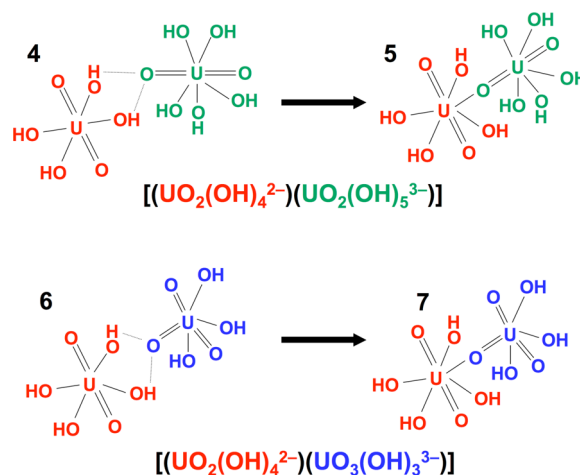
[a]The Gibbs energy differences between the precursor and successor at different levels of theory are given in Table 2.

the inner-sphere complex was formed via U−O_{yl}−U bond formation (4 → 5). All of our attempts to optimize the structure of binuclear complexes with hydroxo bridge(s) failed. Such complexes are probably unstable, and only oxo bridging was found to be feasible. Odoh et al.[20] studied the structures of $(UO_2)_2(OH)_n^{4-n}$ complexes in the gas phase for $n = 2−6$ at the DFT, MP2, and CCSD(T) levels. They found the hydroxo bridge to be stable for $n = 2$, 4, and 6, whereas an oxo bridge was more stable for $n = 3$ and 5. Odoh et al. concluded that the stability is largely dominated by the coordination number of uranium atoms, and it appeared that an oxo bridge was preferred when the complex had an odd number of hydroxyl ligands. In our case, we found the oxo bridge to be far more stable for $n = 9$ (odd number) in agreement with the gas-phase calculations by Odoh et al. In the case of $[(UO_2(OH)_4^{2-})$-$(UO_3(OH)_3^{3-})]$, the bridging between two uranium atoms was assumed to take place via the third oxo oxygen atom in $UO_3(OH)_3^{3-}$ because this oxygen had a longer U−O distance than U−O_{yl} and also a higher affinity to another uranium (6 → 7). The energy of the inner-sphere complexes 5 and 7 relative to the outer-sphere precursors 4 and 6, respectively, are given in Table 2.

As can be seen in Table 2, the reaction energies of 4 → 5 and 6 → 7 transitions are diverging with theories. However, the reaction energy to form a binuclear complex is overall lower for

Table 2. Gibbs Reaction Energies of 4 → 5 and 6 → 7 in Scheme 2 in kJ mol^{-1}

	4 → 5	6 → 7
M06-2X	+34.0	−8.2
B3LYP	+60.1	+31.1
BP86	+55.2	+35.4
MP2 with B3LYP geometry[a]	+32.1	+14.6

[a]The Gibbs energy corrections were taken from the results at the B3LYP level.

$[(UO_2(OH)_4^{2-})(UO_3(OH)_3^{3-})]$ than for $[(UO_2(OH)_4^{2-})$-$(UO_2(OH)_5^{3-})]$ at all levels of theory. Together with the fact that $UO_3(OH)_3^{3-}$ is more stable than $UO_2(OH)_5^{3-}$ (hence favoring the formation of precursor **6** over precursor **4**), the formation of **7** is likely to be favored over **5** because both the energy of the precursor and the reaction energy is lower for **6** → **7**. However, we could not identify a transition state that directly connects **6** and **7**. Clearly, there are several intermediate states that can connect **6** and **7**.

We have also estimated the Gibbs energy to form the outer-sphere complex **6** from the two negatively charged ions $UO_2(OH)_4^{2-}$ and $UO_3(OH)_3^{3-}$. In order to take into account the effect of a strong ionic strength, we used the following formula given by Morel and Hering[21] instead of simply taking the B3LYP energy.

$$K = \frac{4000\pi N_A a^3}{3} \exp\left(\frac{-Z_M Z_L e^2}{4\pi\varepsilon_0\varepsilon kTa}\right) \exp\left(\frac{Z_M Z_L e^2 \kappa}{4\pi\varepsilon_0\varepsilon kT(1+\kappa a)}\right) \quad (1)$$

where κ is the Debye−Hückel ion atmosphere parameter

$$\kappa = \sqrt{\frac{2000e^2 N_A I}{\varepsilon_0\varepsilon kT}} \quad (2)$$

with the constants N_A (Avogadro's constant) = 6.022×10^{23} mol^{-1}, e (elementary charge) = 1.602×10^{-19} C, ε_0 (vacuum permittivity) = 8.854×10^{-12} J^{-1} C^2 m^{-1}, and k (Boltzmann's constant) = 1.381×10^{-23} J K^{-1}. The relative permittivity ε of the medium is 78.54 for water at 25 °C. The parameter a is the closest approach of the ions, which was assumed to be 5×10^{-10} m. An absolute temperature T of 298.15 K, ionic strength I of 3.0, and ion charges $Z_M Z_L$ of +6 have been used. We obtained a log K value of −1.47 from which the ΔG for the formation of complex **6** from $UO_2(OH)_4^{2-}$ and $UO_3(OH)_3^{3-}$ was estimated to be +8.4 kJ mol^{-1}. This value will later be used in Scheme 5 to estimate the activation barrier of the entire pathway.

In the following, we assume that complex **7** is energetically accessible, and the likeliness of the "yl"−oxygen exchange reaction through this complex is studied in the next subsection.

Proton Transfer in $[(UO_2(OH)_4^{2-})(UO_3(OH)_3^{3-})]$ Studied by Quantum-Chemical Calculations. For the results presented above, we conclude that complex **7** is likely to be formed as an energetically accessible intermediate. We focus here on how complex **7** can transform into another complex that can be a precursor for the "yl"−oxygen exchange.

In Scheme 3, we show how complex **7** can go through structural rearrangement and subsequent deprotonation. The first step is a twisting of two uranyl planes so that in the ensuing complex **8** the two uranyl planes are perpendicular to each other. The energy difference between complexes **7** and **8** is very small. At all levels of theory, the energy difference between the

Scheme 3. Structural Rearrangement and Deprotonation in Complex 7[a]
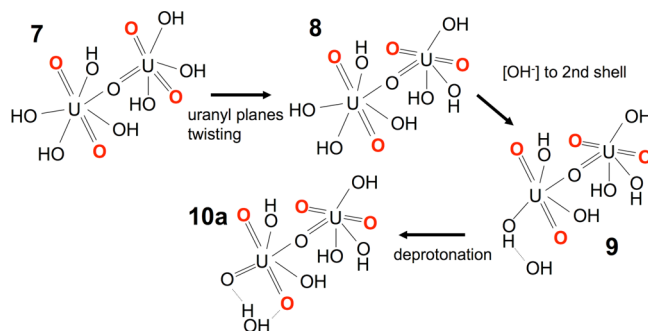
[a]The final complex **10a** is the precursor complex for oxygen exchange (proton transfer). The relative Gibbs energies of these complexes at various levels of theory are given in Table 3.

two complexes is not greater than 2.1 kJ mol^{-1} (Table 3, second and third columns), indicating that complex **7** can easily

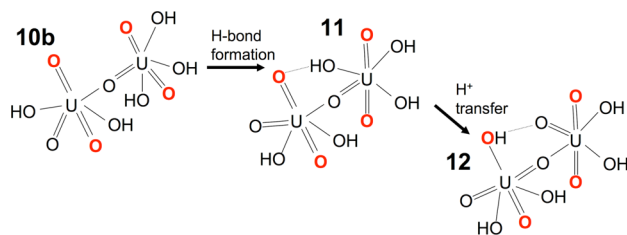**Table 3. Relative Gibbs Energy of the Complexes in Scheme 3[a]**

	7	8	9	10a
M06-2X	0.0	−2.1	−21.6	−2.0
B3LYP	0.0	+1.2	−14.8	−29.7
BP86	0.0	+1.4	−26.6	−45.4
MP2 with B3LYP geometry[b]	0.0	−0.5	−24.4	−27.8

[a]The energy is relative to complex **7** in kJ mol^{-1}. [b]The Gibbs energy corrections were taken from the results at the B3LYP level.

transform into complex **8**. The following step is a loss of one hydroxo ligand from the first shell that enters into the second coordination sphere (complex **9**). An energy of −16 to −28 kJ mol^{-1} for the exergonic reaction **8** → **9** is consistently found in all theories used. It is clear that complex **9** is more stable than complex **8**. Finally, deprotonation of complex **9** yields complex **10a**. The reaction energy of **9** → **10a** varies between the highest value of +19.6 kJ mol^{-1} (M06-2X) and the lowest of −18.8 kJ mol^{-1} (BP86). However, all theories give rather similar results with negative reaction energy except for M06-2X. As discussed earlier, M06-2X underestimates the stability of the complex with increased oxo bonds. This implies that M06-2X tends to overestimate the reaction energy of **9** → **10a**. When the MP2 energy with B3LYP geometry was used, the reaction **7** → **8** → **9** → **10a** always went downward in energy. In complex **10a**, there are six oxo oxygen atoms surrounding two uranium atoms. Uranium on the left-hand side in complex **10a** of Scheme 3 is surrounded by four oxo groups. It can be assumed that these oxo groups are better proton acceptors than those in dioxouranium(VI) and they can contribute to a faster proton transfer/oxygen exchange.

We now come to the second part of proton transfer in the dimer complex. The pathway is depicted in Scheme 4, and the corresponding energies are given in Table 4. The starting complex **10b** is essentially the same as **10a** shown in Scheme 3, but the second-shell water is omitted (**10a** − H_2O = **10b**). In this scheme, the first step is an intramolecular hydrogen-bond formation between OH and oxo (**10b** → **11**). The energy difference between complexes **10b** and **11** is small (−11.0 to +6.1 kJ mol^{-1}) and concerns only the formation of a new hydrogen bond. The next step is proton transfer from OH to

Scheme 4. Proton Transfer in Complex 10b, Which Has the Stoichiometry $[(UO_3(OH)_2)^{2-}(UO_3(OH)_3)^{3-}]^a$

^{a}The relative Gibbs energy of these complexes at various levels of theory are given in Table 4.

Table 4. Relative Gibbs Energy and Gibbs Energy of Activation of the Complexes in Scheme 4^a

	10b	11	TS^a	12
M06-2X	0.0	−2.1	+37.6	+26.3
B3LYP	0.0	+6.1	+37.3	+21.0
BP86	0.0	−11.0	---	---^{c}
MP2 with B3LYP geometry^b	0.0	+0.4	+30.5	+10.8

^{a}Transition states between **11** and **12**. ^{b}Gibbs energy corrections were taken from the results at the B3LYP level. ^{c}Structure optimization did not converge. The energy is relative to complex **10b** in kJ mol^{-1}.

uranyl oxo (**11 → 12**), which is the key step in the entire pathway. For this reaction, we were not able to get the structure of **12** at the BP86 level. However, we obtained the structures at the M06-2X and B3LYP levels. The reaction energy for **11 → 12** was overall low, considering the fact that this reaction involves uranyl−oxo bonds. The lowest reaction energy is +7.0 kJ mol^{-1} at the MP2 level (with B3LYP geometry), and the highest is +28.4 kJ mol^{-1} at the M06-2X level. Again, M06-2X gives the highest energy presumably because of the involvement of oxo bonds.

Because the proton-transfer reaction **11 → 12** is one of the key steps in the entire pathway, we identified the transition state between complexes **11** and **12**. The activation Gibbs energy (relative to the energy of complex **10b**) for proton transfer is +37.6 and +37.3 kJ mol^{-1} at the M06-2X and B3LYP levels, respectively (Table 4). At the MP2 level using the B3LYP geometry, the same reaction has an activation energy of +30.5 kJ mol^{-1}. The entire reaction in Scheme 4 is characterized by an activation barrier of about 30−40 kJ mol^{-1}. However, in the preceding Scheme 3, the final product (complex **10a**) has a Gibbs energy of approximately 30 kJ mol^{-1} lower than that of the precursor complex. Therefore, when we look at the entire pathway through **7−12**, the energy of the transition state cannot largely exceed that of the precursor. Once the binuclear complex **7** is formed, it can rather easily react to complex **12** in which exchange of the OH$^-$ ligand and OH$^-$ in water takes place and the oxygen exchange reaction is completed.

Comparison with Previously Proposed Oxygen Exchange Mechanisms. Szabó and Grenthe studied the "yl"−oxygen exchange in an alkaline solution using NMR spectroscopy.[6] They concluded that the "yl"−oxygen exchange takes place via the binuclear species $[(UO_2(OH)_4^{2-})(UO_2(OH)_5^{3-})]$. However, in their study, it was assumed that hydrolysis of $UO_2(OH)_4^{2-}$ yields $UO_2(OH)_5^{3-}$. If hydrolysis of $UO_2(OH)_4^{2-}$ results in $UO_3(OH)_3^{3-}$ instead of $UO_2(OH)_5^{3-}$, the stoichiometry of the binuclear species should

be better written as $[(UO_2(OH)_4^{2-})(UO_3(OH)_3^{3-})]$. Our quantum-chemical calculations as well as XAS data suggest that hydrolysis of $UO_2(OH)_4^{2-}$ indeed yields $UO_3(OH)_3^{3-}$. Quantum-chemical calculations also confirmed that the binuclear species $[(UO_2(OH)_4^{2-})(UO_3(OH)_3^{3-})]$ is energetically accessible and can be a precursor for the "yl"−oxygen exchange.

Furthermore, according to Szabó and Grenthe, the activation Gibbs energy of the "yl"−oxygen exchange reaction in an alkaline solution is 60.8 ± 2.4 kJ mol^{-1}. We estimated the activation Gibbs energy of the "yl"−oxygen exchange via $[(UO_2(OH)_4^{2-})(UO_3(OH)_3^{3-})]$, assuming that the rate-dominating step is proton transfer between oxygen atoms, namely, the reaction **11 → 12** in Scheme 4. Assuming also that the Gibbs energies obtained by quantum-chemical calculations are additive, we obtained the activation Gibbs energy of the "yl"−oxygen exchange through the formation of $[(UO_2(OH)_4^{2-})(UO_3(OH)_3^{3-})]$ to be +64.7, +55.2, and +22.9 kJ mol^{-1} at the B3LYP, M06-2X, and B3LYP/MP2 levels, respectively. The activation energy obtained at the B3LYP/MP2 level is much lower than the experimental value. One source of error is the use of the B3LYP structure but calculating the energy at the MP2 level. However, we also found that the B3LYP/MP2 reaction energy depends heavily on the number of correlated electrons. In all MP2 calculations in Table 1−4, we used the frozen-core approximation and U 5s/5p/5d and O 1s electrons were kept frozen during the correlation energy calculations. However, when only O 1s electrons were frozen, the reaction energy substantially dropped by about 15 kJ mol^{-1}. The validity of the MP2 method has been disputed for the water exchange reaction of the uranyl(VI) aquo ion in which "yl"−oxygen atoms stay chemically inert.[22] For the reactions involving "yl"−oxygen, the validity of MP2 is more disputable and needs to be tested especially from the aspect of the electron correlation and multireference character of the system. However, this is beyond the scope of the present investigation where the focus was on the speciation, chemical reactions, and dynamics. Once again we point out that a reasonable agreement between the theoretical and experimental results was found at the B3LYP level in this study and also in the previous studies.[5,10] The entire pathway and its energetics at the B3LYP level are depicted in Scheme 5.

We also compared the energetics of the dimer scenario with those of the previously proposed monomer mechanism. The transition state of the intramolecular proton transfer within complex **3** has been identified (corresponding to reaction 3a by Shamov and Schreckenbach[5]), and the activation Gibbs energy was found to be 118.3 kJ mol^{-1} (Scheme S1 in the SI). For the same reaction, Shamov and Schreckenbach obtained a much lower activation Gibbs energy of 65 kJ mol^{-1} using the PBE functional for gas-phase calculations. After the addition of the Gibbs energy to form complex **3** (17.6 kJ mol^{-1}), we get an activation Gibbs energy of 135.9 kJ mol^{-1} for proton transfer in a monomer scenario, which is substantially higher than that obtained for the binuclear scenario (64.7 kJ mol^{-1}) using the same level of theory.

In summary, our present results confirm the "yl"−oxygen exchange mechanism through the binuclear scenario proposed by Szabó and Grenthe and later affirmed by Harley et al..[7] Together with the fact that the "yl"−oxygen exchange of uranyl(VI) in an acidic solution also occurs via a binuclear complex,[4c,9,10] it seems that the formation of an U−O$_{yl}$−U

Scheme 5. Entire Pathway of the Uranyl(VI) "yl"−Oxygen Exchange and Gibbs Energy Change[a]
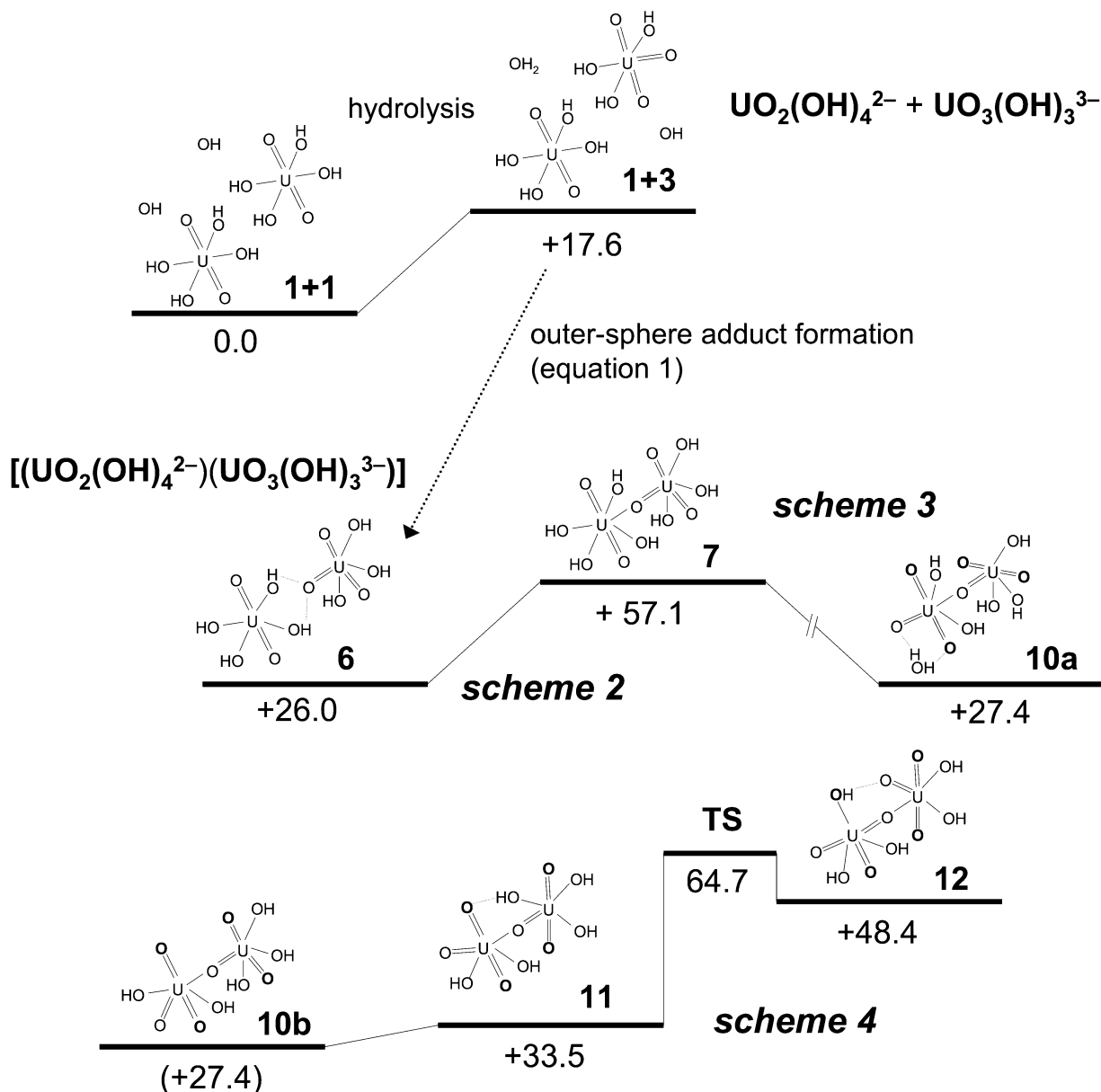
[a]The pathway consists of hydrolysis, dimer complex formation, structural reorganization, and proton transfer. The energies obtained at the B3LYP level are given in kJ mol⁻¹ assuming **10a** and **10b** are energetically equivalent.

bridge plays a key role in facilitating proton shuttling, thereby leading to faster "yl"−oxygen exchange.

CONCLUSIONS

We found experimental and theoretical evidence that supports the presence of an uranium(VI) species in solution with three U−O oxo bonds. The presence of this species $(UO_3(OH)_3^{3-})$ has been postulated earlier in the theoretical work by Shamov and Schreckenbach. Our combined experimental and theoretical study suggests that the species $UO_2(OH)_5^{3-}$, reported in earlier experimental work, are, in fact, more likely to be $UO_3(OH)_3^{3-}$.

We further studied by quantum-chemical calculations the mechanism of exchange between oxygen of uranyl(VI) and that of the hydroxo ligand. We assumed the binuclear adduct $[(UO_2(OH)_4^{2-})(UO_3(OH)_3^{3-})]$ to be the key species for the

oxygen exchange in a strong alkaline solution. We also assumed that the rate-limiting step is the proton-transfer reaction. DFT calculations showed that this binuclear species is energetically accessible, and an intramolecular proton-transfer pathway within this complex was further explored. Our assumptions are corroborated by identification of the realistic "yl"−oxygen exchange pathway via $[(UO_2(OH)_4^{2-})(UO_3(OH)_3^{3-})]$, which has an activation Gibbs energy close to the experimental value by Szabó and Grenthe. Although Szabó and Grenthe concluded that the key species is $[(UO_2(OH)_4^{2-})(UO_2(OH)_5^{3-})]$, the difference from our results can be explained by the fact that $UO_2(OH)_5^{3-}$ and $UO_3(OH)_3^{3-}$ are indistinguishable by potentiometry.

THEORETICAL AND EXPERIMENTAL SECTION

Quantum-Chemical Calculations. Calculations were performed in an aqueous phase using the *Gaussian 09* program[23] employing the

DFT method (M06-2X,[24] B3LYP,[25] and BP86[26]) as well as MP2 through the use of a conductorlike polarizable continuum model.[27] The energy-consistent small-core effective core potential and the corresponding basis set suggested by Dolg et al.[28] were used for uranium. The most diffuse basis functions on uranium with the exponent 0.005 (all s, p, d, and f type functions) were omitted as in previous studies.[29] For oxygen and hydrogen, the valence triple-ζ plus polarization basis was used.[30] The 1s shell of oxygen and 5s, 5p, and 5d shells of uranium were kept frozen during correlation energy calculation at the MP2 level. The Gibbs energy correction to the electronic energy was calculated at the same level from the vibrational energy levels in the aqueous phase and the molecular partition functions. The structures were confirmed to be energy minima through vibrational frequency analysis, where no imaginary frequency was found to be present. The transition states were identified through a single imaginary frequency that describes the translation movement across the energy barrier. The spin−orbit effects and basis set superposition error corrections were neglected. Using the same methodology, we successfully studied proton-transfer reactions in uranyl(VI) complexes in previous studies.[10,31] The coordinates of all complexes, including those of the transition states at the B3LYP level, are given in the SI.

Sample Preparation. $UO_2(NO_3)_2 \cdot 6H_2O$ (Merck, Germany) was heated to obtain UO_3. The test solutions **S1** and **S5** were prepared from appropriate amounts of UO_3 and tetramethylammonium hydroxide (TMA-OH; Sigma-Aldrich) under an inert gas atmosphere to get a final total concentration of 50 mM UO_2^{2+} and 1.0 or 3.0 M TMA-OH for **S1** and **S5**, respectively. For sample **S1**, solids were dissolved in ultrapure water (Milli-Q), whereas for sample **S5**, the solids were dissolved in methanol. Each TMA-OH molecule contains five water molecules so that the methanol concentration in **S5** is approximately 75 vol %. The test solutions were kept in the dark under a N_2 atmosphere. Both solutions were filled into the appropriate polyethylene sample holders.

XAS. XAS measurements were performed at the Rossendorf Beamline (ROBL) of the European Synchrotron Radiation Facility in Grenoble, France.[32] Sample **S1** was recorded at room temperature. Sample **S5** was measured at 200 K in a closed-cycle helium cryostat using a water-cooled Si(111) double-crystal monochromator in channel cut mode (5−35 keV). The U L_{III}-edge spectrum was recorded in transmission mode. The energy scale was calibrated using the maximum of the first derivative of the K-edge spectrum of yttrium (17038 eV), which was simultaneously measured with each spectrum. The EXAFS spectra were analyzed according to standard procedures using *EXAFSPAK*.[33] Theoretical scattering phases and amplitude functions were calculated with the ab initio calculation program *FEFF8*.[34] Theoretical simulation of U L_{III}-edge XANES spectra were performed using the *FEFF9* program[35] for the molecules $UO_2(OH)_4^{2-}$ and $UO_2(OH)_5^{3-}$ using the B3LYP structures within the real-space full multiple-scattering and self-consistent-field approach.

ASSOCIATED CONTENT

Ⓢ Supporting Information

Experimental versus theoretical vibrational frequency of the O=U=O symmetric stretching vibration, k^3-weighted U L_{III}-edge EXAFS spectra of uranium(VI) samples and corresponding Fourier transforms, proton transfer mechanism through mononuclear scenario, and coordinates of all complexes obtained at the B3LYP level. This material is available free of charge via the Internet at http://pubs.acs.org.

AUTHOR INFORMATION

Corresponding Author

*E-mail: S.Tsushima@hzdr.de.

Notes

The authors declare no competing financial interest.

REFERENCES

(1) Clark, D. L.; Conradson, S. D.; Donohoe, R. J.; Keogh, D. W.; Morris, D. E.; Palmer, P. D.; Rogers, R. D.; Tait, C. D. *Inorg. Chem.* **1999**, *38* (7), 1456−1466.

(2) Arnold, P. L.; Patel, D.; Wilson, C.; Love, J. B. *Nature* **2008**, *451* (7176), 315−317.

(3) (a) Arnold, P. L.; Hollis, E.; White, F. J.; Magnani, N.; Caciuffo, R.; Love, J. B. *Angew. Chem., Int. Ed.* **2011**, *50* (4), 887−890. (b) Arnold, P. L.; Pecharman, A. F.; Hollis, E.; Yahia, A.; Maron, L.; Parsons, S.; Love, J. B. *Nat. Chem.* **2010**, *2* (12), 1056−1061. (c) Arnold, P. L.; Pécharman, A. F.; Love, J. B. *Angew. Chem., Int. Ed.* **2011**, *50*, 9456−9458. (d) Arnold, P. L.; Jones, G. M.; Odoh, S. O.; Schreckenbach, G.; Magnani, N.; Love, J. B. *Nat. Chem.* **2012**, *4*, 221−227. (e) Brown, J. L.; Wu, G.; Hayton, T. W. *J. Am. Chem. Soc.* **2010**, *132* (21), 7248−7249. (f) Fortier, S.; Hayton, T. W. *Coord. Chem. Rev.* **2010**, *254* (3−4), 197−214. (g) Fortier, S.; Kaltsoyannis, N.; Wu, G.; Hayton, T. W. *J. Am. Chem. Soc.* **2011**, *133*, 14224−14227. (h) Hayton, T. W.; Wu, G. *Inorg. Chem.* **2009**, *48* (7), 3065−3072.

(4) (a) Schreckenbach, G.; Hay, P. J.; Martin, R. L. *Inorg. Chem.* **1998**, *37* (17), 4442−4451. (b) Hratchian, H. P.; Sonnenberg, J. L.; Hay, P. J.; Martin, R. L.; Bursten, B. E.; Schlegel, H. B. *J. Phys. Chem. A* **2005**, *109* (38), 8579−8586. (c) Szabó, Z.; Grenthe, I. *Inorg. Chem.* **2007**, *46* (22), 9372−9378.

(5) Shamov, G. A.; Schreckenbach, G. *J. Am. Chem. Soc.* **2008**, *130* (41), 13735−13744.

(6) Szabó, Z.; Grenthe, I. *Inorg. Chem.* **2010**, *49* (11), 4928−4933.

(7) Harley, S. J.; Ohlin, C. A.; Johnson, R. L.; Panasci, A. F.; Casey, W. H. *Angew. Chem., Int. Ed.* **2011**, *50* (19), 4467−4469.

(8) Clark, D. L.; Conradson, S. D.; Donohoe, R. J.; Gordon, P. L.; Keogh, D. W.; Palmer, P. D.; Scott, B. L.; Tait, C. D. *Inorg. Chem.* **2013**, *52* (7), 3547−3555.

(9) Mashirov, L.; Mikhalev, V.; Suglobov, D. *C. R. Chim.* **2004**, *7* (12), 1179−1184.

(10) Tsushima, S. *Inorg. Chem.* **2012**, *51* (3), 1434−1439.

(11) (a) Bühl, M.; Schreckenbach, G. *Inorg. Chem.* **2010**, *49* (8), 3821−3827. (b) Bühl, M.; Kabrede, H. *ChemPhysChem* **2006**, *7* (11), 2290−2293. (c) Wåhlin, P.; Danilo, C.; Vallet, V.; Real, F.; Flament, J. P.; Wahlgren, U. *J. Chem. Theory Comput.* **2008**, *4* (4), 569−577. (d) Wåhlin, P.; Vallet, V.; Wahlgren, U.; Grenthe, I. *Inorg. Chem.* **2009**, *48* (23), 11310−11313.

(12) (a) Bühl, M.; Wipff, G. *ChemPhysChem* **2011**, *12* (17), 3095−3105. (b) Tsushima, S. *J. Phys. Chem. A* **2007**, *111* (18), 3613−3617.

(13) Moll, H.; Reich, T.; Szabo, Z. *Radiochim. Acta* **2000**, *88* (7), 411−415.

(14) Quilès, F.; Nguyen-Trung, C.; Carteret, C.; Humbert, B. *Inorg. Chem.* **2011**, *50* (7), 2811−2823.

(15) Wahlgren, U.; Moll, H.; Grenthe, I.; Schimmelpfennig, B.; Maron, L.; Vallet, V.; Gropen, O. *J. Phys. Chem. A* **1999**, *103* (41), 8257−8264.

(16) Le Naour, C.; Trubert, D.; Di Giandomenico, M. V.; Fillaux, C.; Den Auwer, C.; Moisy, P.; Hennig, C. *Inorg. Chem.* **2005**, *44* (25), 9542−9546.

(17) Ikeda, A.; Hennig, C.; Tsushima, S.; Takao, K.; Ikeda, Y.; Scheinost, A. C.; Bernhard, G. *Inorg. Chem.* **2007**, *46* (10), 4212−4219.

(18) (a) Ikeda, A.; Hennig, C.; Rossberg, A.; Tsushima, S.; Scheinost, A. C.; Bernhard, G. *Anal. Chem.* **2008**, *80* (4), 1102−1110. (b) Lucks,

C.; Rossberg, A.; Tsushima, S.; Foerstendorf, H.; Scheinost, A. C.; Bernhard, G. *Inorg. Chem.* **2012**, *51* (22), 12288−12300.

(19) Schreckenbach, G.; Shamov, G. A. *Acc. Chem. Res.* **2010**, *43* (1), 19−29.

(20) Odoh, S. O.; Govind, N.; Schreckenbach, G.; de Jong, W. A. *Inorg. Chem.* **2013**, *52* (19), 11269−11279.

(21) Morel, F. M. M.; Hering, J. G. *Principles and Applications of Aquatic Chemistry*, 1st ed.; Wiley-Interscience: New York, 1993.

(22) (a) Rotzinger, F. P. *Chem.—Eur. J.* **2007**, *13* (3), 800−811. (b) Vallet, V.; Wahlgren, U.; Grenthe, I. *Chem.—Eur. J.* **2007**, *13* (36), 10294−10297. (c) Rotzinger, F. P. *Chem.—Eur. J.* **2007**, *13* (36), 10298−10302.

(23) Frisch, M. J.; Trucks, G. W.; Schlegel, H. B.; Scuseria, G. E.; Robb, M. A.; Cheeseman, J. R.; Scalmani, G.; Barone, V.; Mennucci, B.; Petersson, G. A.; Nakatsuji, H.; Caricato, M.; Li, X.; Hratchian, H. P.; Izmaylov, A. F.; Bloino, J.; Zheng, G.; Sonnenberg, J. L.; Hada, M.; Ehara, M.; Toyota, K.; Fukuda, R.; Hasegawa, J.; Ishida, M.; Nakajima, T.; Honda, Y.; Kitao, O.; Nakai, H.; Vreven, T.; Montgomery, J. A., Jr.; Peralta, J. E.; Ogliaro, F.; Bearpark, M.; Heyd, J. J.; Brothers, E.; Kudin, K. N.; Staroverov, V. N.; Kobayashi, R.; Normand, J.; Raghavachari, K.; Rendell, A.; Burant, J. C.; Iyengar, S. S.; Tomasi, J.; Cossi, M.; Rega, N.; Millam, J. M.; Klene, M.; Knox, J. E.; Cross, J. B.; Bakken, V.; Adamo, C.; Jaramillo, J.; Gomperts, R.; Stratmann, R. E.; Yazyev, O.; Austin, A. J.; Cammi, R.; Pomelli, C.; Ochterski, J. W.; Martin, R. L.; Morokuma, K.; Zakrzewski, V. G.; Voth, G. A.; Salvador, P.; Dannenberg, J. J.; Dapprich, S.; Daniels, A. D.; Farkas, Ö.; Foresman, J. B.; Ortiz, J. V.; Cioslowski, J.; Fox, D. J. *Gaussian 09*, revision A.1; Gaussian Inc.: Wallingford, CT, 2009.

(24) Zhao, Y.; Truhlar, D. G. *J. Phys. Chem. A* **2006**, *110* (15), 5121−9.

(25) (a) Becke, A. D. *J. Chem. Phys.* **1993**, *98* (7), 5648−5652. (b) Lee, C. T.; Yang, W. T.; Parr, R. G. *Phys. Rev. B* **1988**, *37* (2), 785−789.

(26) (a) Becke, A. D. *Phys. Rev. A* **1988**, *38* (6), 3098−3100. (b) Perdew, J. P. *Phys. Rev. B* **1986**, *33* (12), 8822−8824.

(27) (a) Barone, V.; Cossi, M. *J. Phys. Chem. A* **1998**, *102* (11), 1995−2001. (b) Cossi, M.; Rega, N.; Scalmani, G.; Barone, V. *J. Comput. Chem.* **2003**, *24* (6), 669−681.

(28) Küchle, W.; Dolg, M.; Stoll, H.; Preuss, H. *J. Chem. Phys.* **1994**, *100* (10), 7535−7542.

(29) Tsushima, S. *Dalton Trans.* **2011**, *40*, 6732−6737.

(30) Krishnan, R.; Binkley, J. S.; Seeger, R.; Pople, J. A. *J. Chem. Phys.* **1980**, *72* (1), 650.

(31) (a) Tsushima, S. *Inorg. Chem.* **2009**, *48* (11), 4856−4862. (b) Tsushima, S.; Brendler, V.; Fahmy, K. *Dalton Trans.* **2010**, *39* (45), 10953−10958.

(32) Matz, W.; Schell, N.; Bernhard, G.; Prokert, F.; Reich, T.; Claussner, J.; Oehme, W.; Schlenk, R.; Dienel, S.; Funke, H.; Eichhorn, F.; Betzl, M.; Prohl, D.; Strauch, U.; Huttig, G.; Krug, H.; Neumann, W.; Brendler, V.; Reichel, P.; Denecke, M. A.; Nitsche, H. *J. Synchrotron Radiat.* **1999**, *6*, 1076−1085.

(33) George, G. N.; Pickering, I. J. *EXAFSPAK*; Stanford Synchrotron Radiation Laboratory, Stanford Linear Accelerator Center: Stanford, CA, 2000.

(34) Ankudinov, A. L.; Ravel, B.; Rehr, J. J.; Conradson, S. D. *Phys. Rev. B* **1998**, *58* (12), 7565−7576.

(35) Rehr, J. J.; Kas, J. J.; Vila, F. D.; Prange, M. P.; Jorissen, K. *Phys. Chem. Chem. Phys.* **2010**, *12* (21), 5503.